Zhang *et al. Microstructures* 2024;4:2024051
DOI: 10.20517/microstructures.2024.29

Microstructures

Research Article

Open Access

A molecular dynamics assisted insight on damping enhancement in carbon fiber reinforced polymer composites with oriented multilayer graphene oxide coatings

Muhan Zhang[1], Yalin Yu[2], Li Li[3], Helezi Zhou[1], Luyang Gong[1], Huamin Zhou[1]

[1]State Key Laboratory of Material Processing and Die & Mold Technology, School of Materials Science and Engineering, Huazhong University of Science and Technology, Wuhan 430074, Hubei, China.
[2]Aerospace Research Institute of Materials & Processing Technology, Beijing 100076, China.
[3]State Key Laboratory of Intelligent Manufacturing Equipment and Technology, School of Mechanical Science and Engineering, Huazhong University of Science and Technology, Wuhan 430074, Hubei, China.

Correspondence to: Assoc. Prof. Helezi Zhou, School of Materials Science and Engineering, Huazhong University of Science and Technology, 1037, Luoyu Road, Hongshan District, Wuhan 430074, Hubei, China. E-mail: Helezizhou@hust.edu.cn; Prof. Huamin Zhou, School of Materials Science and Engineering, Huazhong University of Science and Technology, 1037, Luoyu Road, Hongshan District, Wuhan 430074, Hubei, China. E-mail: Hmzhou@hust.edu.cn

How to cite this article: Zhang M, Yu Y, Li L, Zhou H, Gong L, Zhou H. A molecular dynamics assisted insight on damping enhancement in carbon fiber reinforced polymer composites with oriented multilayer graphene oxide coatings. *Microstructures* 2024;4:2024051. https://dx.doi.org/10.20517/microstructures.2024.29

Received: 27 Mar 2024 **First Decision:** 6 Jun 2024 **Revised:** 14 Jun 2024 **Accepted:** 20 Jun 2024 **Published:** 13 Aug 2024

Academic Editor: Zaiping Guo **Copy Editor:** Fangling Lan **Production Editor:** Fangling Lan

Abstract

Fiber-reinforced polymer composites with high damping performance have been required in diverse applications. The interlayer slip characteristics of the graphene family offer a clear benefit in enhancing the damping performance of materials. In this study, an oriented graphene oxide (GO) structure was designed on the carbon fiber surface to enhance the damping capacity of the composites. The molecular dynamics method was proposed to investigate the damping mechanism of multilayer GO-reinforced polymer composites based on energy dissipation, which is consistent with the results revealed by dynamic mechanical analysis. Under a wide range of loading strain, vibration frequency, and temperature, GO induces a higher loss factor/lower quality factor of the composite materials. The visualization of the atomic displacement field demonstrates that the sliding of multilayer GO during vibration enhances the mutual friction among polymer segments, leading to a pronounced increase in the energy loss. Notably, substantial enhancements in damping properties were observed with thicker GO coatings.

This is due to the fact that the uniformly distributed shear stresses are more likely to activate interlayer slip, and higher frictional forces consume more mechanical energy.

Keywords: Carbon fiber, graphene oxide, damping properties, interlayer slip, energy dissipation, molecular dynamics simulation

INTRODUCTION

In the contemporary landscape of escalating performance requisites spanning diverse engineering domains, carbon fiber reinforced polymer (CFRP) composites have attained prominence as omnipresent composite materials in high-end industries, primarily attributable to their extremely elevated mechanical properties, commendable chemical stability, low thermal expansion coefficient, and superlative designability[1]. Nowadays, the imperative to conceive composite components endowed with superior damping characteristics assumes a pivotal role in mitigating composite damage and surmounting challenges associated with noise or vibration[2]. Diverging from conventional structural materials such as metals, polymer-based composites manifest heightened absorption of shock-induced energies, owing to their augmented capacity for energy dissipation. Consequently, scientific research and engineering applications remain captivated by the advancement and production of high-damping composite materials[3,4].

Broadly, the foundational tenet governing energy dissipation in fiber-reinforced composites predominantly orbits the viscoelastic nature intrinsic to the fiber/matrix constituents or manifests through inelastic and irreversible phenomena, such as damage or plasticity, with a particular emphasis on damping induced by interfacial interactions[5,6]. The incorporation of one- or two-dimensional carbon nanofillers into the composite matrix has proven to be a discerning approach for enhancing damping characteristics, owing to their inherent self-lubricating attributes and the facile induction of a stick-slip effect on contact surfaces[7-10]. Empirical investigations have unveiled that the incorporation of a specific mass ratio of carbon nanotubes (CNTs) engenders an approximate 100% augmentation in the modal damping ratio of composite beam structures[11]. Additionally, heightened energy dissipation is achieved through the mutual sliding of the inner surfaces of multi-walled CNTs (MWCNTs) when subjected to small dynamic strains[12,13]. In contrast to CNT/MWCNT, the graphene family exhibits substantial promise in enhancing structural damping across both low-frequency (10-250 Hz) and high-frequency (> 1 MHz) vibration environments[14-16]. The planar configuration of graphene endows it with significantly greater flexibility than CNTs, thereby influencing stick-slip/slip mechanisms within nanomaterials[17]. Moreover, owing to the low interlayer shear force and low surface energy of graphene materials, the interaction between friction pairs can be effectively transformed into interlayer sliding of graphene during interface friction, thereby reducing adhesion and friction on various substrates[18,19]. Lu *et al.* revealed through quasi-static/dynamic damping tests that the loss factor of polyurethane-based composites with a sandwich structure modified by graphene oxide (GO) coatings increased by ~71% and ~94% compared to pure polyurethane, respectively[7]. Rafiee *et al.*, employing vibration testing, evaluated the damping effects in multi-scale GO/glass fiber/epoxy composites and observed an increase in the damping ratio with higher GO nanoparticle content[20]. Pan *et al.* further illustrated that the maximum first-order loss factor of epoxy-based nanocomposite beams reinforced with graphene nanoplatelets was 62.2% higher than that of CNTs[21]. Moreover, a novel orientation-based GO interface developed in our previous work can result in a remarkable 113% increase in the damping loss factor of CFRP[22].

Despite their paramount significance, the intricate mechanisms governing damping capacity have hitherto been subject to limited scholarly inquiry. The microscopic-level exploration of the damping properties of CFRPs modified with carbon nanoparticles remains largely uncharted. In recent decades, advances in

extremely powerful computer hardware and software have empowered molecular dynamics (MD) simulations to delve into the structure-performance relationships of materials[23]. The MD technique offers a distinct advantage in comprehending the interactions among minute molecules, systematically elucidating the fundamental mechanisms governing damping properties in both inorganic[24,25] and organic[26-28] material systems by constructing amorphous cells. Within the realm of composite materials, a multitude of damping mechanisms arises from diverse material combinations and structural designs. For instance, Zhu *et al.* discovered that the coupling effect of intermolecular friction/interaction significantly influences damping parameters[29]. Qiao *et al.* ascertained that hydrogen-bonded frameworks generated inside the system can constrict the free motion space of polymer chains, thereby enhancing damping properties by increasing internal friction and energy dissipation that disrupt H-bonds[30]. Jiang *et al.* confirmed that raising the mismatch of elastic modulus near the contact interface and/or extending the interfacial region can effectively improve the loss factor[31]. Additionally, amplifying the energy dissipation of materials is also regarded as a fundamental strategy to attain a heightened damping capacity[32-34]. Current studies have provided preliminary insights into the advantageous effects of graphene materials on the damping behavior of composites from a molecular perspective[35-38]. Specifically, by employing coarse-grained MD and nanomechanical investigations, Wei *et al.* demonstrated that the energy dissipation capability of multilayer GO can be restored subsequent to interfacial slip[38]. While existing knowledge acknowledges the role of graphene in enhancing damping capacity, a conspicuous lacuna exists in the realm of in-depth investigations into the mechanisms underpinning the improvement of the damping performance of CFRP modified by GO. Consequently, our work seeks to fill this void and provide a comprehensive understanding of these mechanisms.

In this study, we delved into the impact of GO on the damping response of CFRP using experimental and computational simulation techniques. The *in-situ* construction of GO coating on the carbon fiber (CF) surface was achieved through electrophoretic deposition (EPD) techniques, and CFRP samples were subsequently prepared using vacuum-assisted resin transfer molding (VARTM). The damping loss factor of CFRPs with different strains, frequencies, temperatures, and coating thicknesses was measured using a dynamic mechanical analyzer (DMA). By developing a comprehensive atomic model of the epoxy/CF-GO interface, we analyzed the parameter dependence of energy dissipation in characteristic structures and comprehensively evaluated the microstructural damping capacity through the derivation of the quality factor (Q). In addition, the interlayer slip behaviors on CF surfaces modified with various GO sheets were examined, encompassing theoretical surface stress distribution, interaction mechanisms, energy fluctuations, interface friction, and the transition from intralayer to interlayer slippages, aiming to elucidate the potential mechanisms by which 2D carbon nanomaterials enhance damping performance.

EXPERIMENTAL AND COMPUTATIONAL STRATEGY

Materials

The woven fabrics comprised CFs (T300, 3K, and diameter of about 7 μm) with an areal density of 200 g/m^2, as provided by the Toray Industries (Tokyo, Japan). The epoxy resin (Araldite LY 1564) and the hardener (Aradur 22962) were bought from Huntsman Advanced Materials (USA). Few- and multilayer GO (1-5 layers and 6-10 layers, respectively) were provided by the Xiamen Knano Graphene Technology Co., Ltd (Xiamen, China).

Electrophoretic deposition of GO

In the beginning, the raw carbon fabrics were bathed in acetone for 48 h at 25 °C to remove the sizing agents. For the EPD of GO on the CF, the fabric was entangled in parallel on a fixed-size aluminum alloy frame and used as the anode, and two copper plates were used as the cathode. Each fabric and copper plate was placed with 20 mm of facing distance in acrylic fixtures. EPD was carried out under a constant voltage

of 25 V for 30 min with the assistance of an ultrasonic treatment (60 W, 40 kHz). The GO concentration was 0.25 g/L and the pH of GO-water suspension was adjusted to 10.0 by adding 0.1 M sodium hydroxide. After the deposition, fabrics were dried at 90 °C for 12 h. It should be noted that both few- and multilayer GO on the CF surface were deposited using the same EPD parameters.

Preparation of CFRP composites

GO-coated CF fabrics were used as the base material to synthesize the CFRP composites. Firstly, 12 plies of fabrics following the $[0°]_{12}$ lay-up with a nominal thickness of 3.55 mm were prepared. Then, dry fabrics were infiltrated with a mixture of epoxy and curing agent at a weight ratio of 100:25 using VARTM. After the impregnating process driven by vacuum negative pressure, the composites were cured at 78 °C for 8 h. Note that the volume fraction of CFRP samples ranged from 55%-60%, and the void volume content of the laminate was ~0.2%. The entire process of sample preparation above is shown in Figure 1. Especially, The CFRP prepared using the T300 as received was named @$CFRP_{CG}$, the sample prepared using the desized CF was named @$CFRP_{Desized}$, and the composite prepared using the GO-coated CF was named @$CFRP_{GO\ (i\ Layers)}$, respectively (i = 1-5 or 6-10).

Characterization methods

Morphology characterization

Surface morphologies and element distribution of carbon fabrics were characterized using a JEOL JSM7600F field emission scanning electron microscopy (FESEM, 10 kV) equipped with an energy dispersive spectrometer (EDS).

Damping test

Damping describes the tendency of a material to reduce oscillation amplitude in an oscillating system. Herein, the damping properties of CFRP were examined by DMA with the aid of a TA Q800 instrument (New Castle, Delaware, USA). Three conditional sweep tests, including strain, frequency, and temperature sweep, were carried out, from which the damping loss factor was extracted from composites modified with few layers GO, as summarized in Table 1. The effect of few/multiple layers GO on the damping characteristics was also investigated at a constant dynamic strain of 0.018%, a vibration frequency of 1 Hz, and a temperature of 20 °C. All testing was done with a 3-point bending mode based on 50.0 mm × 10.0 mm × 1.0 mm DMA specimens. At least three samples for each group were tested and the average values were taken.

Simulation methods

Molecular dynamics models

In this research, the classic composite structure was composed of an epoxy polymer, a GO layer, and a CF substrate, as shown in Figure 2A. The epoxy molecule was formed by the cross-linking process of diglycidyl ether of bisphenol A (DGEBA) monomer and triethylenetetramine (TETA) monomer, which represents the basic type of epoxy in CFRP. Considering the limitations of computing ability, a representative *in-situ* cross-linked epoxy unit, consisting of 180 molecules of DGEBA and 60 molecules of TETA, was constructed with a target density of 1.2 g/cm^3. During the cross-linking process, three reactive sites of TETA were connected to three DGEBA molecules with a cross-link ratio of 0.5. The C-O bonds in each epoxide group need to be destroyed to form a reactive -CH_2 site that can be cross-linked with TETA molecules. After that, the epoxy cell was subjected to a combined equilibration approach to alleviate the structural distortions and the residual stress, which consists of a series of geometry optimization steps and a 500 ps-equilibration in canonical (NVT) ensemble under 300 K (The energy optimization results are shown in Supplementary Figure 1).

Table 1. The test conditions of DMA under three sweep modes

	Strain sweep	Frequency sweep	Temperature sweep
Strain	0.10%-0.20%	0.018%	0.018%
Frequency	1 Hz	0.1-200 Hz	1 Hz
Temperature	20 °C	20 °C	-25-100 °C

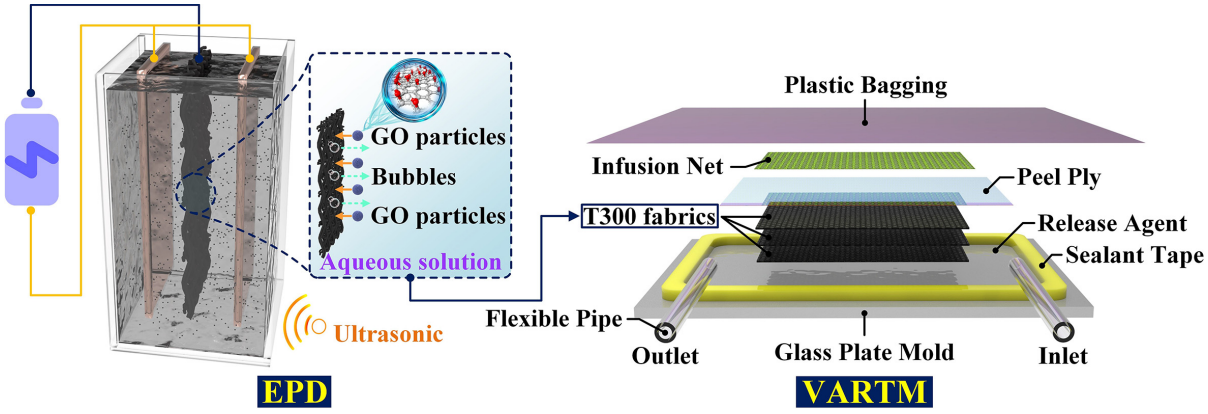

Figure 1. Schematic of steps in EPD and CFRP laminate making through a VARTM method.

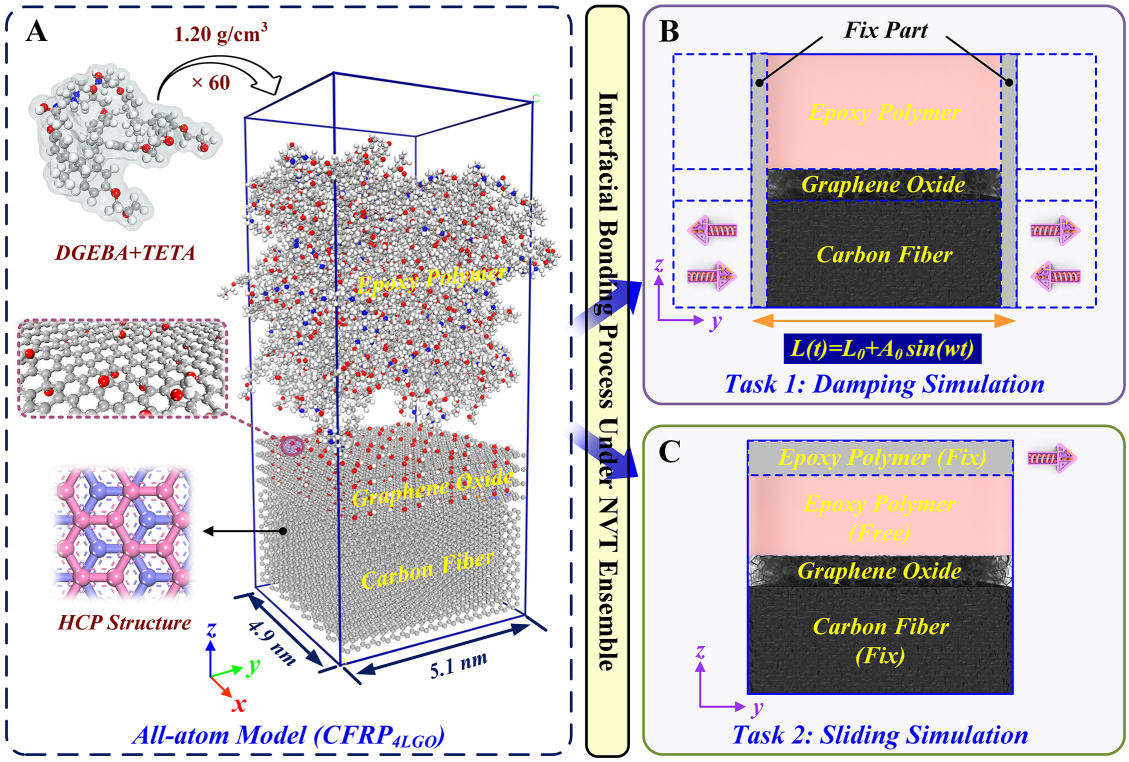

Figure 2. (A) Atomic configurations of the GO-modified CFRP system and schematics of the (B) damping and (C) sliding simulations.

The GO model was obtained by several GO sheets separated individually by a distance of 3.4 Å which periodically duplicate the graphite unit with the cell parameters of a = 2.48 Å, b = 4.39 Å, c = 3.4 Å and

α= 90°, β = 90°, γ = 90°. Besides, oxygen-containing (hydroxyl and epoxy) functional groups were randomly distributed on both sides of GO sheets, which achieves ~25% C_{sp3}/C_{total}. The final multilayer GO structure in a size of 4.9 nm × 5.1 nm was generated. To represent pristine CF, 15 perpendicular graphene layers that parallel to each other with a close-packed hexagonal structure and 3.4 Å spacing were created. The bond length between carbon atoms from each graphite unit was initially set to 1.42 Å. Meanwhile, the partial atomic charges of CF atoms were set to zero. The modeling of the substrate structure above was guided by previous investigations[39].

Potentials

We obtain the damping capacity of materials by loading a tensile mode parallel to the *y*-axis direction onto the CFRP system. The interlayer sliding behavior of GO layers intervention on the CF/epoxy interface was also studied. The interactions among carbon atoms in GO have been described by the Universal Force Field (UFF) atomic potentials[40], since it has been successfully used for simulations of GO materials[41]. The electrostatic potential of GO was taken from the atomic point charge model calculated by Stauffer *et al.*[42]. The consistent valence force field (CVFF), which has been demonstrated to correctly predict the mechanical and physical properties of fiber-reinforced polymer composites[43-46], was chosen to model the epoxy molecules in this work. Finally, the interactions between GO and epoxy are described by the Lennard-Jones 12-6 potential. All calculations were performed using the large-scale atomic/molecular massive parallel simulator (LAMMPS)[47]. For non-bonded interaction, the van der Waals (vdW) and short-range electrostatic interactions were cut off at a terminated distance of 10 Å. Simulation details are given as follows.

Interfacial bonding

To achieve sufficient adhesion between polymer molecules and the CF-GO surfaces, structures of all the molecular models were first equilibrated using the isothermal-isobaric (NPT) ensemble at a constant temperature of 300 K for 20 ps (Δt = 1 fs), and the Nosé-Hoover thermostat was applied to control the temperature. Then, the geometry of the entire system was optimized within the NVT ensemble at 300 K over a duration of 200 ps.

Periodic oscillation

Structures were first put into a NVE ensemble for 1 ns with a temperature of 300 K (Δt = 1 fs). Subsequent to the equilibration, the damping simulations were conducted under the NVE ensemble. The single-degree-of-freedom vibration of CFRP was realized by periodically changing the length of the structure along the *y*-axis with a specific amplitude A_0 and angular frequency ω, as described in Figure 2B. Especially, to ensure that the oscillations remain within a linear response regime, the maximum strain ($\varepsilon_{max} = \frac{A_0}{L_0}$) of the box is limited to 2%. Free boundary conditions were employed to avoid the over-constraint induced by periodic mirrored images. For simplicity, the model involved in damping simulation was named D-$CFRP_{i\text{LGO}}$, where *i* means the number of GO layers.

Interlayer sliding

In order to study the long-distance slip characteristics of multilayer GO structures, an interlayer sliding process based on the NVT ensemble was performed. A portion of the epoxy layer at the top, as well as the CF substrate, were regarded as a rigid body separately while the GO sheets and the remaining epoxy molecules were left unconstrained, as shown in Figure 2C. During the sliding simulations, interlayer slip occurred between GO sheets in which the rigid polymer was displaced at a constant average velocity (0.01 nm/ps) in the y direction to slide for 1 ns. Additionally, owing to the limitations of computing resources, a periodic boundary condition was applied in the *-y* axis to simulate a long sliding distance and

sample the sufficient space phase. For simplicity, the model involved in sliding simulation was named S-CFRP$_{i\text{LGO}}$, where *i* means the number of GO layers.

RESULTS AND DISCUSSION

Surface morphology analysis

Figure 3 shows typical scanning electron microscopy (SEM) micrographs of various CF surfaces, and the weight percentage of O, C elements displayed comes from the energy dispersive spectrometry (EDS) area scan. Initially, compared with the control group (CG, Figure 3A and B), the desized CF [Figure 3C and D] exhibited a rough surface with narrow grooves distributed along the longitudinal direction. The removal of the sizing layer, following the treatment with acetone solution, results in a decrease in the oxygen atom content on the fiber surface. After the treatment with the EPD approach assisted by ultrasonics, GO sheets were homogeneously coated on the CF surface, leading to a higher proportion of oxygen element, and the rough wrinkles on the coating surface could be clearly observed, as indicated in Figure 3E-H. Additionally, we observed with an increase in the number of GO layers, the fiber surface tended to develop a film structure with a larger sheet diameter. Furthermore, some gaps between fiber monofilaments were filled by such a thin film, forming a bridge-shaped coating.

Damping properties of the CFRPs

The dynamic mechanical behavior of the CFRPs was thoroughly studied, and the corresponding damping loss factors are depicted in Figure 4, which represents the ratio of loss modulus to the storage modulus. The data presented in Figure 4A-C is cited from our previous work[22], with six points displayed in each sweep mode, which exclude the signals from the test platform or structural resonances.

As observed in Figure 4A-C, tanδ exhibited a gradual increase in CFRPs modified with GO layers compared to @CFRP$_{CG}$ and @CFRP$_{Desized}$ under various external conditions. It confirms that the introduction of GO on the fiber surface significantly enhances the dissipation capacity of composites, possibly due to the improved uniform stress distribution under the influence of nanomaterial characteristics[48]. Regarding the influence of loading conditions on structural damping, the loss factor of all three types of CFRPs maintained a positive correlation with strain and vibration frequency except for @CFRP$_{CG}$ within the low-frequency range (0-40 Hz). However, the relationship between tanδ and the temperature preceding T_g varied for each composite. The loss factors of @CFRP$_{CG}$ and @CFRP$_{Desized}$ showed no sensitivity to temperature, whereas @CFRP$_{GO\text{-}CF}$ exhibited a trend of initially decreasing and then increasing.

Figure 4D illustrates the loss factor of composites modified by GO with different layers on the CF surface. As evident, tanδ of @CFRP$_{GO\ (1\text{-}5\ Layers)}$ increased from 0.0292 (CG) to 0.0327 (+12.0%), while the loss factor of @CFRP$_{GO\ (6\text{-}10\ Layers)}$ grew from 0.0292 to 0.0366 (+25.3%), which further emphasizes the potential of GO, particularly multilayer GO, in enhancing the damping performance of CFRP materials. The onset of interfacial slip of GO/polymer needs to overcome the covalent bond interactions, as GO layers are solely linked by weak forces such as van der Waals and electrostatic interactions. Consequently, with an increase in the number of GO layers, interfacial slipping is more likely to be triggered by external energies, allowing composites to generate higher energy dissipation[49]. On the other hand, as mentioned above, the extensive bridge-shaped coating created by multilayer GO can also increase the slip area between GO interlayers, thereby aiding materials in rapidly dissipating external energy.

Microscopic damping capacity

Parameter dependence of energy dissipation

Many methods exist for evaluating damping in different contexts, including logarithmic decrement, the damping ratio, the specific damping capacity, loss factor, and quality factor *Q*. These indicators for damping

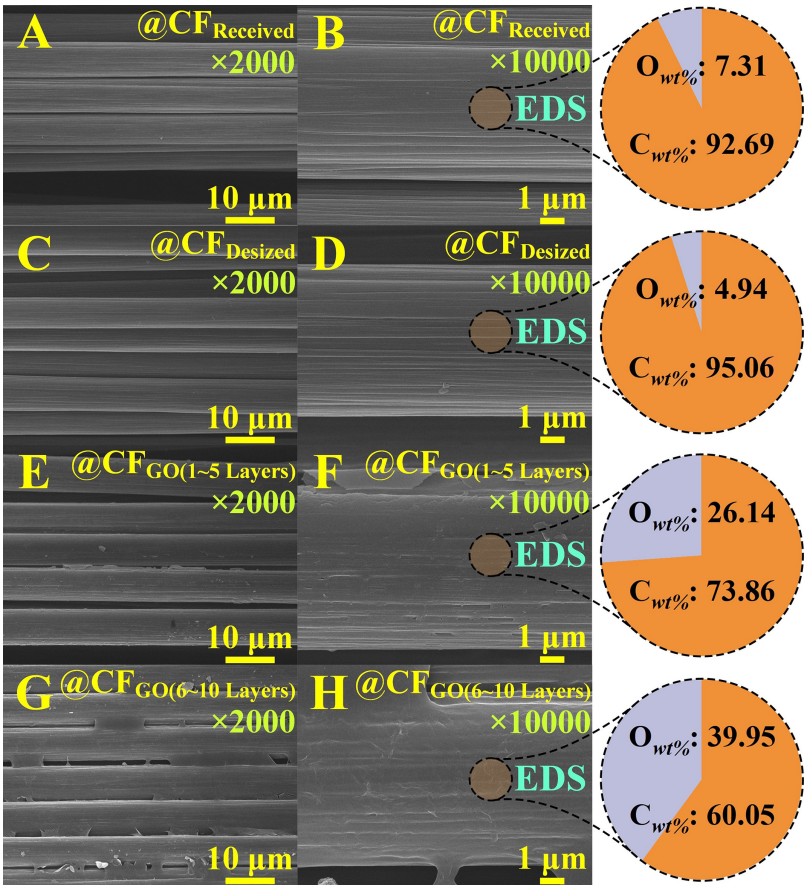

Figure 3. The surface morphology analysis by SEM image investigations and EDS mapping results of (A and B) T300 CF as received, (C and D) desized CF, (E and F) EPD treated CF with 1-5 layers of GO, (G and H) EPD treated CF with 6-10 layers of GO.

performance are applicable under various conditions. Specifically, Q is a dimensionless parameter that signifies the rate at which energy stored in the resonant mode dissipates in the nanoscale[32,33]. The Q can be determined by the ratio of energy stored in the system to the energy dissipated per oscillation cycle:

$$Q = 2\pi \frac{U_{stored}}{U_{disp}} = 2\pi \frac{U_{stored}}{U_{epoxy}+U_{substrate}} \quad (1)$$

where U_{stored} is the maximum strain energy stored in the CFRP system and U_{disp} is the energy dissipated during one oscillation cycle (the energy difference at the initial and the end stage per cycle), which equal to the sum of the energy dissipated in the epoxy cell (U_{epoxy}) and in the CF-GO ($U_{substrate}$). In MD calculations, U_{stored} needs to require the assistance of strain energy, the maximum value of which can be expressed as follows:

$$U_{stored} = \frac{1}{2} V E \varepsilon_0^2 \quad (2)$$

where V and E are the volume and the elastic modulus along the y-axis of the composite system, respectively, and ε_0 indicates the magnitude of strain during one vibrational cycle (ε_0 = 0.02 was considered here). In this study, the elastic modulus was obtained using a classical uniaxial tensile deformation MD

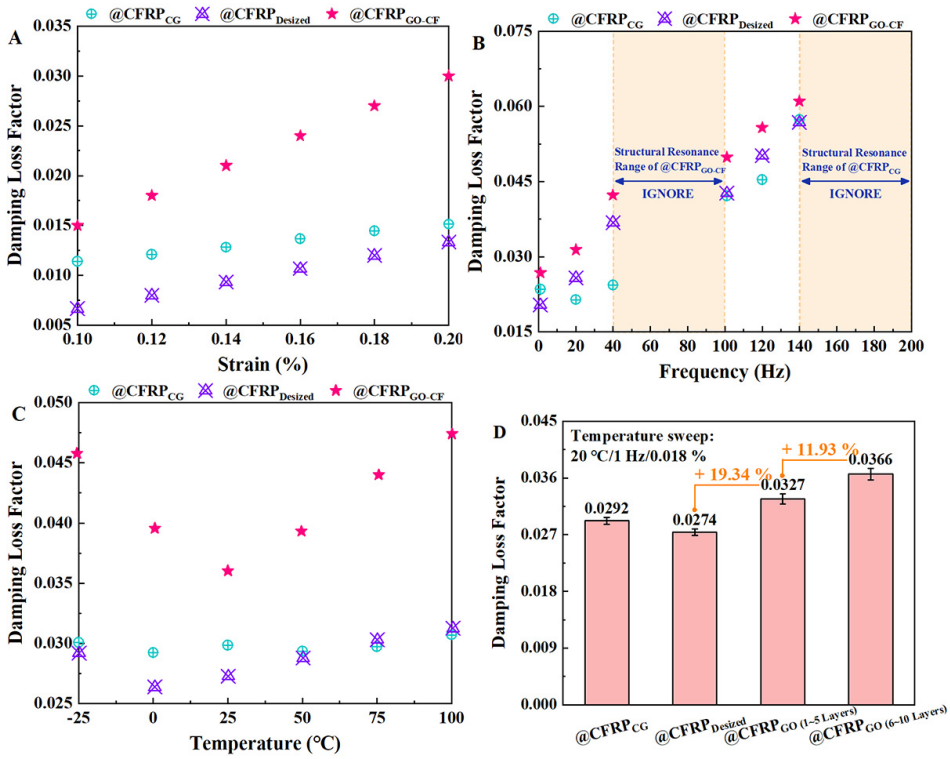

Figure 4. DMA results (tanδ) of CFRP composites under three conditional sweep modes: (A) strain sweep[22], (B) frequency sweep[22], and (C) temperature sweep[22]. (D) Comparison of damping performance between @CFRP$_{CG}$, @CFRP$_{Desized}$ and specimens modified with few- and multilayer GO.

where only a small strain (loading rate of 2×10^{-4} ps^{-1}) in the y-axis direction was set to be nonzero. Specially, E is defined as the ratio of stress perturbation ($d\sigma^*$) to strain perturbation ($d\varepsilon^*$) in the initial linear elastic region of the constitutive curve.

Based on the perspective of continuum mechanics, multiphase composite structures undergo elastic deformation during vibration, leading to energy dissipation within the material. Figure 5A exhibits the variation of the total energy dissipation as a function of the vibration cycles (n) for different CFRP systems. One characteristic of oscillation in a constant energy NVE ensemble is that the energy lost by mechanical motion is converted and stored into internal energy of the system. Thus, the work done on the model will be positive. Herein, the first 100 cycles were selected as the linear fitting region, and the slope was considered as the U_{disp} in per unit. In addition, due to the continuous exchange of excess energy within the system under the effect of the temperature controller, U_{disp} can also equal to the work done by external forces, which is given as:

$$U_{disp} = \frac{\omega}{2\pi T}\int_0^T \sum_n f_0 v_y \cos(\omega t)dt \tag{3}$$

where f_0 is the magnitude of the force applied to each terminal atom in the y direction, v_y is the y component of the atom velocity, T is the total time for which the force is applied, and n is the number of atoms which the external force is applied. As clearly shown, the slope of the curve increases with the number of GO layers, which means that the existence of multilayer GO helps the system dissipate more energy in each

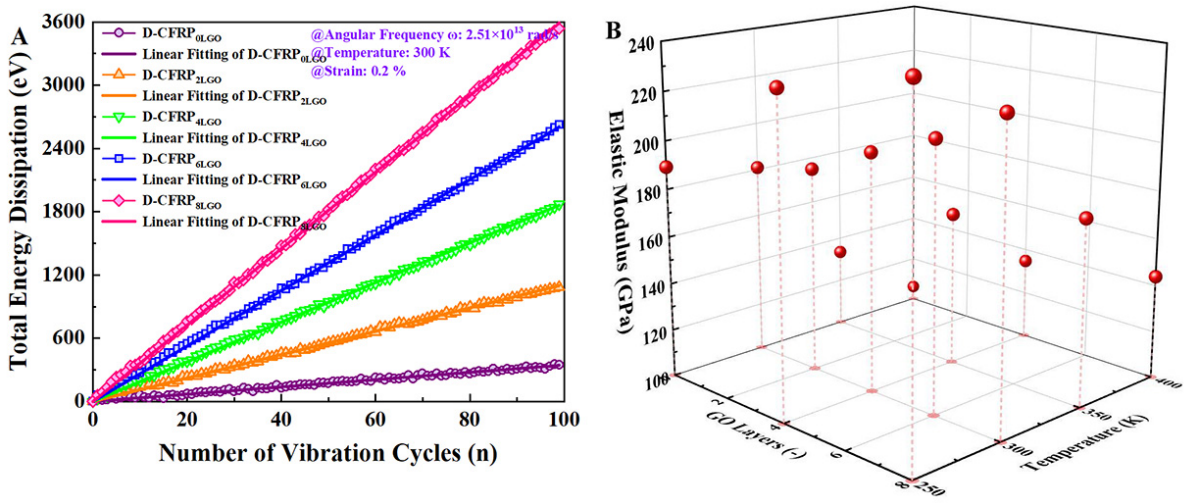

Figure 5. (A) Variation in the total energy of composite systems with cycle number under angular frequency 2.51 × 10^{13} rad/s, temperature 300 K, strain 0.2% and (B) Elastic modulus of composites systems at varied temperatures with different GO layers.

oscillation cycle. Figure 5B shows the elastic modulus versus the temperature and the number of GO layers for CFRP models. As can be seen, the decrease in temperature and the increase in GO layers both increase the elastic modulus of the system. The calculation results are incorporated into Equations (1) and (2) for deriving the *Q*.

Figure 6A-D displays the variation in *Q* factor and U_{disp} with respect to the number of GO layers, cell strain, angular frequency, and temperature, respectively (D-$CFRP_{0LGO}$, D-$CFRP_{4LGO}$, and D-$CFRP_{8LGO}$ were selected as analysis groups). Before the periodic oscillation step, the fundamental stretching frequency of models was obtained by the free vibration method [Supplementary Figure 2]. Based on the fundamental stretching frequency, the angular frequency ranges from 3.14 × 10^{12} to 5.02 × 10^{13} rad/s (corresponding frequency *f*: 0.5-8 THz) was chosen to investigate the frequency effect on damping properties. We confirmed the dependence between the damping performance and the experimental parameters at the microscopic level; that is, the energy dissipation rate increases with higher strain rate, vibration frequency, and temperature, aligning with laboratory findings. Specifically, Figure 6C shows a more significant decline in the *Q* factor compared to other groups. According to the Boltzmann relation ($\overline{K} = 3k_BT/2, k_B = R/N_A = 1.3807 \times 10^{-23} J/K$), it is known that the temperature of atoms is closely related to their motion velocity. With the increase in vibration frequency, the temperature of the simulation system rises, which, in turn, accelerates energy dissipation, resulting in a faster decay of the *Q*. In addition, MD results indicate that under various environmental conditions, the group with multilayer GO (D-$CFRP_{8LGO}$) exhibits a lower *Q* compared to the few-layer GO (D-$CFRP_{4LGO}$) and non-GO coated groups (D-$CFRP_{0LGO}$), suggesting faster energy dissipation mechanisms.

In high-frequency and bulk-mode systems, the uniform distribution of the spatial strain field ultimately limits dissipation through local phonon-phonon scattering, commonly referred to as Akhiezer damping, which is present in all vibrational modes[50]. Generally, under the approximation condition $\omega\tau_{ph} \leq 1$, the *Q* for the Akhiezer damping mechanism can be expressed as:

$$Q^{-1} = \frac{C_p T {\lambda_G}^2}{\rho v^2} \frac{\omega\tau_{ph}}{1 + (\omega\tau_{ph})^2} \quad (4)$$

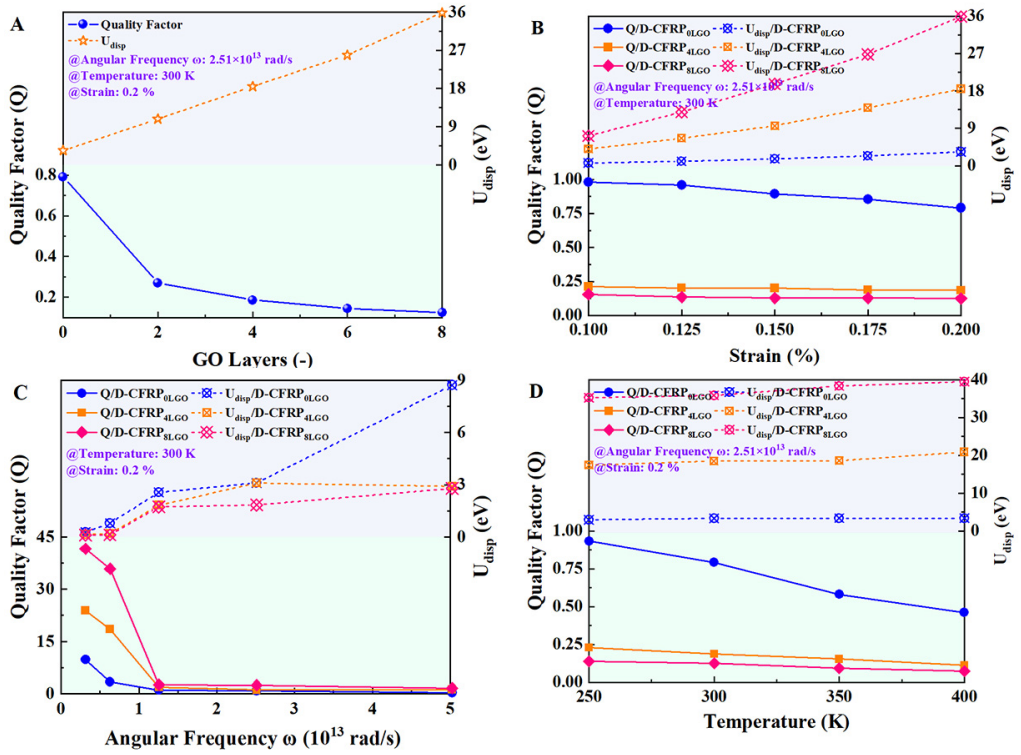

Figure 6. Parameter dependence of Q factor and U_{disp} for CFRP systems: (A) the amount of GO layers, (B) strain magnitude, (C) angular frequency and (D) temperature. The corresponding relationships of (B-D) are captured from D-CFRP$_{0LGO}$, D-CFRP$_{4LGO}$, and D-CFRP$_{8LGO}$.

where C_p the specific-heat capacity, T the temperature, λ_G the Grüneisen parameter, ρ the density of quartz, ω the angular frequency and τ_{ph} the phonon relaxation time. Equation (4) states that, for $\omega\tau_{ph} \leq 1$, Q is scaled as ω^{-1} or T^{-1}. Measurements obtained from our work indicate that as a coating structure is introduced on the fiber surface, the $Q(\omega^{-\alpha})$ or $Q(T^{-\alpha})$ relationship will deviate from the expected $Q(\omega^{-1})$ or $Q(T^{-1})$, and an increase in GO thickness will further enhance this deviation, covering a range from $Q(\omega^{-0.836})$ to $Q(\omega^{-0.570})$ and from $Q(T^{-0.988})$ to $Q(T^{-0.805})$, respectively [Supplementary Figure 3]. In short, as the number of GO layers increases, the dominance of Akhiezer damping gradually diminishes. This complexity arises from the multiple dissipation mechanisms formed by the coupling of internal and external elements such as lattice mismatch, misfit dislocations, interface damping, plastic damping, and thermo-elastic dissipation, which together constitute a complex damping mechanism in the CFRP system.

To elucidate the dissipation behavior of the composites, we track and observe the motion of particles by analyzing the atomic displacement field during the dynamic loading process, as shown in Figure 7. Several representative time points are selected for analysis, including the peak, the valley, and points with an amplitude of zero within a cycle. The snapshot shows that, due to the uneven distribution of polymer chain segments, the regions within the epoxy units where local strain occurs exhibit a high degree of randomness. Unlike D-CFRP$_{0LGO}$, the epoxy resin in D-CFRP$_{8LGO}$ exhibits high-strain areas that shift from fragments to blocks, accompanied by clear visible positive and negative strain differences within the GO layer. It can be understood that the coating structure between resin and fibers acts as a bridge for transmitting energy during periodic vibration. Relative sliding causes the molecules at the interface to vibrate and collide. Following a progressive transfer of this motion to the interior of the matrix, the vibration energy is ultimately dissipated via heat exchange more effectively. Similar views can also be found in the theoretical research of Harrison *et al.* on the surface behavior of crystal materials[51].

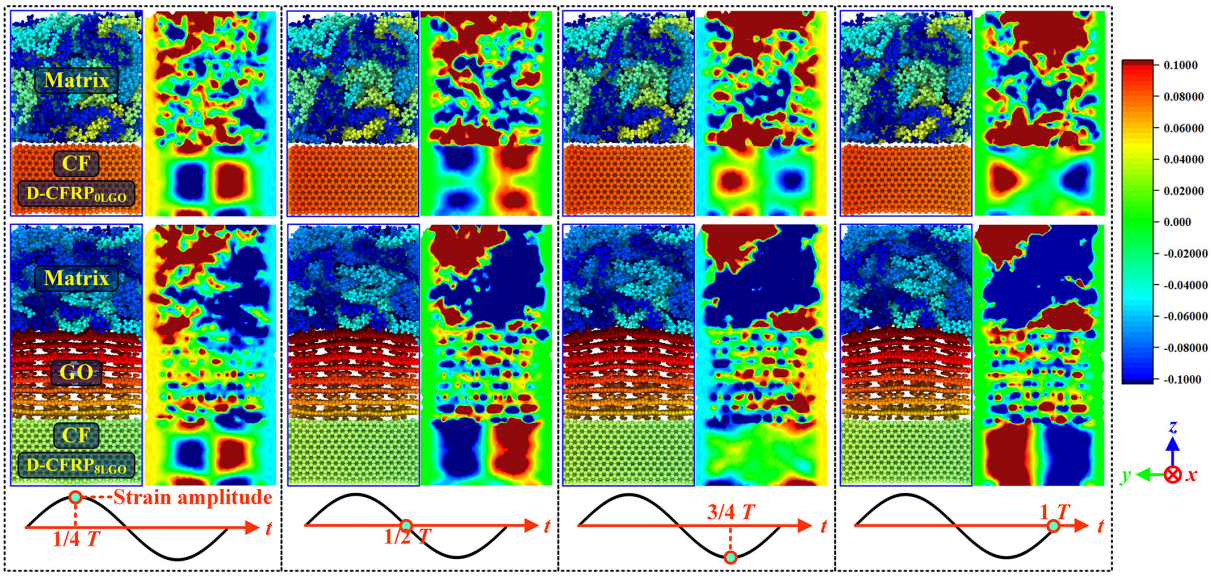

Figure 7. Atomic displacement fields of D-CFRP$_{0LGO}$ and D-CFRP$_{8LGO}$ during one cycle of harmonic vibration (results of 1/4 T, 1/2 T, 3/4 T and T are displayed separately).

Analytical study on surface shear stress distribution

From the perspective of continuum mechanics: CFRP systems will undergo deformation during vibration. Since the layers of the CF-GO and the epoxy are stacked together, the strains formed at the interface of the two continuous layers are coordinated; at the same time, Since the moduli of the CF and the epoxy are different, and a stress jump will occur at the interface. As a "driving force" between the interfaces, this stress jump will cause interface slip, and part of the mechanical energy dissipated at the interface of CFRP systems will be converted into thermal energy. This interface slip process can be modeled using an irreversible diffusive constitutive relation with viscous damping:

$$\tau_{ij} = -\mu_{ijkl}\frac{1}{2}\left(\frac{\partial v_k}{\partial x_l} + \frac{\partial v_l}{\partial x_k}\right) \tag{5}$$

where the four-order tensor μ_{ijkl} is the non-negative viscous (friction) coefficient, τ_{ij} is the viscous (inelastic or friction) stress, v_k is the components of the velocity vector, and x_l is the components of the position vector. The spatial gradient of velocity can be considered as a thermodynamic force, which causes a viscous diffusion process. That is, the viscous stress is the thermodynamic flux. According to the second law of thermodynamics, the rate of entropy generation can be given by:

$$Ts = \mu_{ijkl}\frac{1}{4}\left(\frac{\partial v_k}{\partial x_l} + \frac{\partial v_l}{\partial x_k}\right)\left(\frac{\partial v_i}{\partial x_j} + \frac{\partial v_j}{\partial x_i}\right) \tag{6}$$

where s is the rate of entropy generation, and T is the temperature. For one vibration cycle, the mechanical energy loss U_{disp} in Equation (1) can alternatively as the following form in terms of the irreversible entropy generation rate:

$$U_{disp} = \oint \int_V Ts\, dVdt \tag{7}$$

Recalling that the rate of entropy generation Ts has been defined in Equation (6).

In addition, according to the tribological theory, sliding can also occur when the shear stress between solid surfaces exceeds the static friction of the thin-film structure[52]. By employing a micromechanical model that consists of resin and GO, it has been determined that the aspect ratio of the film structure, which is defined as the length-to-thickness ratio, significantly affects the shear stress distribution between GO sheets. This results in different levels of interfacial slip[53]. The variation of shear stress, τ_y, along the GO/epoxy interface can be expressed as:

$$\tau_y = E_G e_m n \left[\frac{\sinh\left(\frac{ny}{h}\right)}{\cosh\left(\frac{nL}{2h}\right)}\right], n = \sqrt{\frac{2G_m}{E_G}\left(\frac{h}{H}\right)} \tag{8}$$

where E_G is the modulus of GO, e_m is the strain exerted on the epoxy, and L and h are the length and thickness of GO coatings, respectively. H is the thickness of the unit cell, and G_m is the shear modulus of the matrix. The variable y represents the length of a point on the surface of GO from its center, which is limited to $\pm L/2$. To study the influence of the GO aspect ratio on the distribution of shear stress in our model, the assumption is made that all other parameters remain constant, with only the value of L/h undergoing variation. It is worth noting that, in this model, L is defined as $0.34 \times (k - 1)$ nm, where k represents the number of GO sheets. The distribution of surface shear stress is illustrated in Figure 8. For small aspect ratios, the distribution of shear stress becomes more uniform, which is conducive to the generation of interlayer interface slip in GO. Conversely, when the aspect ratio is large, shear stress concentrates at the edge of GO, leading to a reduction in shear stress within the middle region. Therefore, the interlayer slip of composite material units with several layers of GO thin films is more readily activated during vibration. The energy loss can be further enhanced by increased slip distance at the CF/GO interface when the external deformation reaches a larger level.

Interlayer slip and interface friction

Unlike the classical energy dissipation due to the shear deformation of the constrained-layer damping in widely-used macroscale sandwich structures, the energy dissipation mechanism at the microscale is the interlayer slip. Next, the interlayer slip behavior of few-layer/multilayer GO sheets will be explored in detail using the sliding MD simulations.

In this section, sliding MD simulations were carried out to investigate the interlayer slip behavior of few-layer/multilayer GO sheets. It is important to emphasize that the parallel movement of GO sheets described here is an idealized situation assumed for the MD finite unit, which disregards surface wrinkles or clustering of the nanosheets. These factors can still affect interfacial friction or other interactions[7-43]. As shown in Figure 9A-G, we carefully compared physical indicators such as energy, friction, and mean square displacement (MSD) between S-CFRP$_{4LGO}$ and S-CFRP$_{8LGO}$. The movement of atoms during the interaction between GO and epoxy resin or CF significantly influences the bonding strength and durability of the interface. Figure 9B displays the binding energy ($E_{Interaction}$) of the epoxy/substrate and GO/GO interfaces in two groups, encompassing several non-bonded forces such as van der Waals forces and electrostatic interactions. The $|E_{Interaction}|$ between epoxy/substrate in both groups is ~20% higher than GO/GO, suggesting

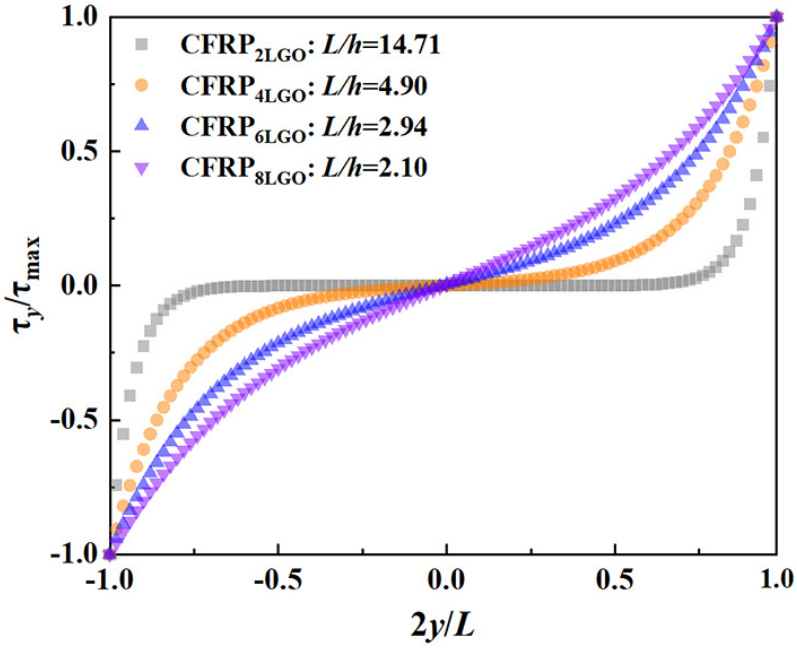

Figure 8. Theoretical distribution of surface shear stress based on different aspect ratios of GO.

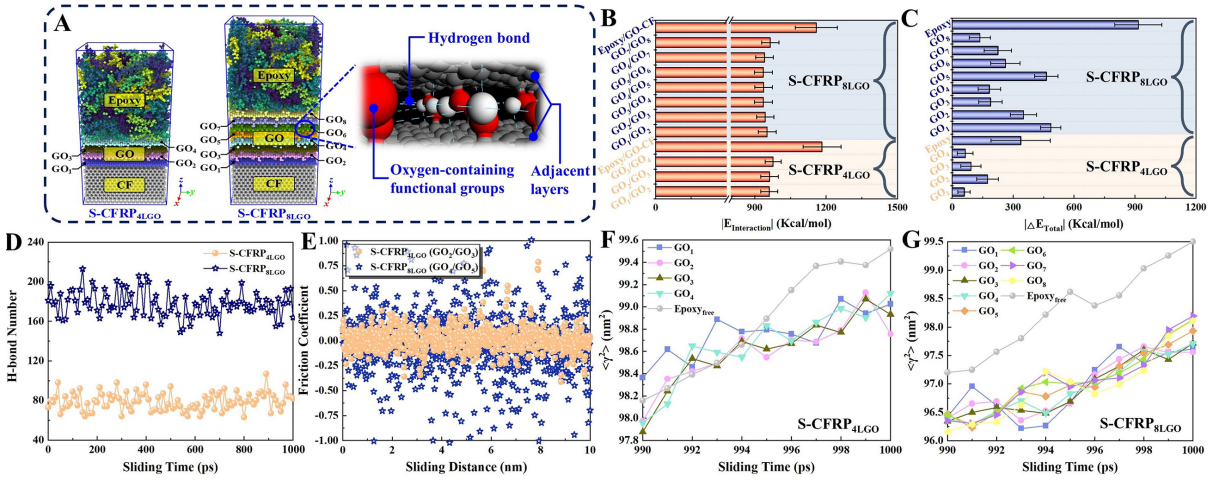

Figure 9. Comparison of interlayer sliding performance between CFRP systems modified with few/multiple layers of GO: (A) Snapshots of the all-atom models for S-CFRP$_{4LGO}$ and S-CFRP$_{8LGO}$, (B) the interfacial interaction energy, (C) the total energy, (D) the number of hydrogen bond, (E) the interface friction coefficient and (F and G) the MSD findings of CFRP unit throughout the last 10-ps sliding simulation.

that the adsorption strength between the GO sheets is weaker, which well explains the phenomenon that the intralayer slippages between epoxy/fiber will preferentially transform into interlayer sliding inside the coating. Due to the continuous detachment, unraveling and stretching of the flexible polymer chains, the energy fluctuations originating from the epoxy units surpass those of the GO sheets following a 1-ns sliding motion of the rigid polymer component. Moreover, the total energy (defined as the sum of kinetic/potential energy) variations of the epoxy or GO layers in S-CFRP$_{8LGO}$ are generally greater than those in S-CFRP$_{4LGO}$, as illustrated in Figure 9C. Observations from the one-dimensional Prandtl-Tomlinson model demonstrate that the energy stored on the solid surface during the sticky sliding phase may not always be fully dissipated

by atomic-scale friction[54]. Hence, a fraction of energy is reintroduced into the system and accumulated in the GO layers, causing energy disparity among adjacent layers.

The polar functional groups linked to the surface of GO promote the creation of a complex hydrogen bonding network between adjacent layers, a strong effect that is constantly broken/formed in real-time with functional group dislocations during interlayer slip. Multilayer GO possesses a larger quantity of hydrogen bonds compared to few-layer GO [Figure 9D], resulting in a more pronounced hysteresis loss in the coating. This disparity in hydrogen bond quantity is a significant factor contributing to the greater divergence in the dynamic friction coefficient between the two groups [Figure 9E]. In short, S-CFRP$_{8LGO}$ demonstrates higher transient friction in its GO layer compared to S-CFRP$_{4LGO}$. Interface friction is primarily caused by interactions between GO layers, including sliding between neighboring layers and atomic interactions within individual sheets. When multiple layers of GO slide against each other, the interactions between their atoms increase friction, which, in turn, causes more heat energy to be released. Meanwhile, studies have demonstrated through the MD approach that the strength and characteristics of interface friction are also closely correlated with the interlayer distance and structural alterations of GO[55].

Figure 9F and G exhibits the MSD results of the CFRP unit during the last 10-ps slip time (rigid CF does not participate in data statistics). Due to the slider being positioned at the top of the polymer, the movement of the sheets away from the polymer bulk is less than that of the epoxy-free part. In addition, the difference in MSD between different layers of GO varies at any time, indicating that interlayer slip behavior is a continuous process accompanied by the formation and development of irregular mutual dislocations between GO sheets. In the viewpoint of classical physics, the shear stress can be approximately evaluated by $\tau = \tau_0 \sin\left(\frac{2\pi d}{a}\right)$, where τ_0 is the magnitude of the shear stress, d is the sliding distance, and a is the equilibrium distance between atoms. As seen, the shear stress is position-dependent or dislocation-dependent, which is confirmed in our MD simulation [Figure 9E]. The displayed dynamic friction coefficient μ of the central layers, is defined as the ratio of tangential force to normal force in adjacent layers during sliding (more information is shown in Supplementary Figure 4). The shear stress can be divided into two parts: elastic stress and inelastic stress (friction). Since the in-plane elastic modulus of GO sheets is far larger than that of their interlayer, the sliding behavior is dominating. Thus, the shear stress can be viewed as friction.

However, it is worth noting that the increase in interfacial friction may suppress the interlayer slippage displacement of coatings. According to the perspective of classical physics, the energy loss caused by frictional motion maintains a numerical integral relationship with the friction force at the reinforcement surface and the slippage displacement: $\Delta W = \int f(t) d\delta(t)$. Therefore, when the constraint of $f(t)$ on $\delta(t)$ is too high, it might have negative effects on ΔW.

Figure 10 illustrates a schematic diagram of the inter/intra-layer slip mechanisms of epoxy/CF-GO interface structure under damping vibration. The symbol represents interface dislocations occurring during the vibration process. For a small number of GO layers [Figure 10A], comprises three components: the relative displacement $S_{E\text{-}G}$ of the GO/epoxy interface, S_G of the GO/GO interface, and $S_{C\text{-}G}$ of the GO/CF interface [Figure 10B]. In the case of thick GO coatings [Figure 10C], due to the competitive relationship of non-bonded interactions at different interfaces, the relative displacement components S_{G1}, S_{G2}, and S_{G3} at the interlayer GO/GO interface also contribute to the intralayer slippages [Figure 10D]. This means that the intralayer slippages between epoxy/CF partially transform into interlayer slippages inside coatings. Prior research has demonstrated that slide occurring at the interface between GO layers can absorb a higher amount of energy compared to slip at the GO/epoxy interface[56,57], which will endow structural components with better shock-absorbing and noise-reducing functions.

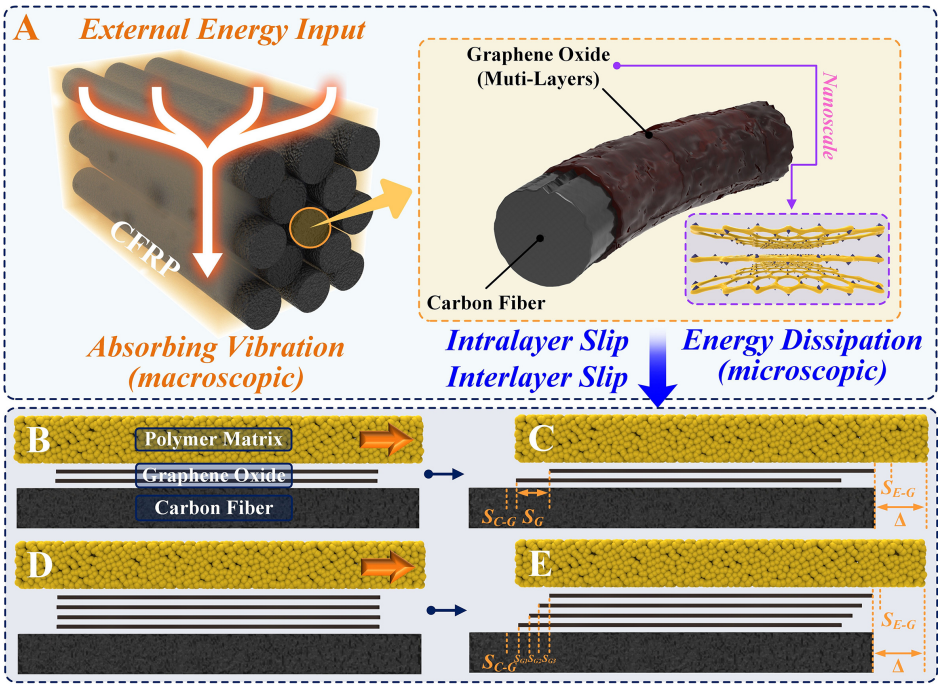

Figure 10. Schematic diagram of interlayer and intralayer slippages of epoxy/CF interfaces guided by GO coating when CFRPs are subjected to external loads: (A) vibration absorption process, (B and C) before/after interface slip of few-layers GO, (D and E) before/after interface slip of multiple-layers GO.

CONCLUSIONS

In summary, we designed and explored a CFRP damping modification method based on *in-situ* construction of oriented GO coatings on CF surfaces. Diverging from conventional views, our work underscored the pivotal role played by the interlayer slip properties of GO nanosheets in modulating energy dissipation rates. The addition of GO-coated fibers significantly improves the energy dissipation rate of composites during vibration. This improvement is consistently observed across a wide range of strain, vibration frequency, and temperature conditions in the DMA test. The visualization of the atomic displacement field indicates that the coating facilitates energy transmission between epoxy and CF, enhancing the extensive development of intermolecular motion among polymer chains. In addition, multilayer GO-modified CFRP exhibits stronger damping ability, increasing the loss factor by up to 25.34% and reducing Q by as much as 82.52%.

Multilayer GO exhibits a more consistent distribution of shear stress on its surface compared to few-layer GO, which facilitates easier activation of interlayer slip. External energy can partially transform intralayer slippages between polymer/CF into interlayer slippages of GO/GO due to competing interfacial interactions. Meanwhile, during the sliding process, the irregular dislocations generated in adjacent sheets induce mechanical energy to be consumed as heat energy through the continuous formation and destruction of hydrogen bond networks and interface friction.

DECLARATIONS

Authors' contributions

Methodology, software, writing-original draft: Zhang M

Formal analysis: Zhang M, Li L
Investigations: Zhang M, Gong L
Data Curation: Yu Y
Conceptualization: Zhou H (Zhou Helezi)
Writing-Reviewing and Editing: Zhou H (Zhou Helezi), Li L
Supervision: Zhou H (Zhou Helezi), Zhou H (Zhou Huamin)
Resources: Zhou H (Zhou Huamin)
Funding acquisition: Zhou H (Zhou Helezi), Zhou H (Zhou Huamin), Li L

Availability of data and materials
Not applicable.

Financial support and sponsorship
This work was financially supported by the National Natural Science Foundation of China (No. 52275336, No. U20A20288).

Conflicts of interest
All authors declared that there are no conflicts of interest.

Ethical approval and consent to participate
Not applicable.

Consent for publication
Not applicable.

REFERENCES
1. Hohe J, Neubrand A, Fliegener S, et al. Performance of fiber reinforced materials under cryogenic conditions - a review. *Compos Part A Appl Sci Manuf* 2021;141:106226. DOI
2. Fasana A, Ferraris A, Polato DB, Airale AG, Carello M. Composite and damping materials characterization with an application to a car door BT - advances in Italian mechanism science. In: Carbone G, Gasparetto A, eds. Advances in Italian Mechanism Science. IFToMM ITALY 2018. Mechanisms and Machine Science. Cham: Springer International Publishing; 2018, pp. 174-84. DOI
3. Sujon MA, Islam A, Nadimpalli VK. Damping and sound absorption properties of polymer matrix composites: a review. *Polym Test* 2021;104:107388. DOI
4. Chung DDL. Structural composite materials tailored for damping. *J Alloys Compd* 2003;355:216-23. DOI
5. Chandra R, Singh SP, Gupta K. Damping studies in fiber-reinforced composites - a review. *Compos Struct* 1999;46:41-51. DOI
6. Gibson RF. Damping characteristics of composite materials and structures. *J Mater Eng Perform* 1992;1:11-20. DOI
7. Lu W, Qin F, Wang Y, et al. Engineering graphene wrinkles for large enhancement of interlaminar friction enabled damping capability. *ACS Appl Mater Interfaces* 2019;11:30278-89. DOI
8. Long WJ, Wei JJ, Xing F, Khayat KH. Enhanced dynamic mechanical properties of cement paste modified with graphene oxide nanosheets and its reinforcing mechanism. *Cem Concr Compos* 2018;93:127-39. DOI
9. Khan SU, Li CY, Siddiqui NA, Kim JK. Vibration damping characteristics of carbon fiber-reinforced composites containing multi-walled carbon nanotubes. *Compos Sci Technol* 2011;71:1486-94. DOI
10. Ashraf T, Ranaiefar M, Khatri S, et al. Carbon nanotubes within polymer matrix can synergistically enhance mechanical energy dissipation. *Nanotechnology* 2018;29:115704. DOI
11. Giovannelli A, Di Maio D, Scarpa F. Industrial-graded epoxy nanocomposites with mechanically dispersed multi-walled carbon nanotubes: static and damping properties. *Materials* 2017;10:1222. DOI PubMed PMC
12. Gardea F, Glaz B, Riddick J, Lagoudas DC, Naraghi M. Identification of energy dissipation mechanisms in CNT-reinforced nanocomposites. *Nanotechnology* 2016;27:105707. DOI PubMed
13. Joy A, Varughese S, Sankaran S, Haridoss P. Role of interface on damping characteristics of multi-walled carbon nanotube reinforced

epoxy nanocomposites. *Mater Res Express* 2019;6:1050c4. DOI

14. Lahiri D, Das S, Choi W, Agarwal A. Unfolding the damping behavior of multilayer graphene membrane in the low-frequency regime. *ACS Nano* 2012;6:3992-4000. DOI PubMed
15. Bunch JS, van der Zande AM, Verbridge SS, et al. Electromechanical resonators from graphene sheets. *Science* 2007;315:490-3. DOI
16. Barton RA, Ilic B, van der Zande AM, et al. High, size-dependent quality factor in an array of graphene mechanical resonators. *Nano Lett* 2011;11:1232-6. DOI
17. Xing C, Zhang M, Liu L, et al. Constructing and regulating nanochannels in two-dimensional-material-based membranes for specified separation applications. *Microstructures* 2023;3:2023031. DOI
18. Min C, Liu D, Shen C, et al. Unique synergistic effects of graphene oxide and carbon nanotube hybrids on the tribological properties of polyimide nanocomposites. *Tribol Int* 2018;117:217-24. DOI
19. Zhang J, Gao X, Xu Q, Ma T, Hu Y, Luo J. Atomistic insights into friction and wear mechanisms of graphene oxide. *Appl Surf Sci* 2021;546:149130. DOI
20. Rafiee M, Nitzsche F, Labrosse MR. Fabrication and experimental evaluation of vibration and damping in multiscale graphene/fiberglass/epoxy composites. *J Compos Mater* 2019;53:2105-18. DOI
21. Pan S, Feng J, Safaei B, Qin Z, Chu F, Hui D. A comparative experimental study on damping properties of epoxy nanocomposite beams reinforced with carbon nanotubes and graphene nanoplatelets. *Nanotechnol Rev* 2022;11:1658-69. DOI
22. Gong L, Zhang F, Peng X, et al. Improving the damping properties of carbon fiber reinforced polymer composites by interfacial sliding of oriented multilayer graphene oxide. *Compos Sci Technol* 2022;224:109309. DOI
23. Peter C, Kremer K. Multiscale simulation of soft matter systems - from the atomistic to the coarse-grained level and back. *Soft Matter* 2009;5:4357-66. DOI
24. Du G, Tan Z, Li Z, et al. Microscopic damping mechanism of micro-porous metal films. *Curr Appl Phys* 2018;18:1388-92. DOI
25. Zhai J, Song X, Xu A, Chen Y, Han Q. Dislocation damping and defect friction damping in magnesium: molecular dynamics study. *Met Mater Int* 2021;27:1458-68. DOI
26. Zhang H, Zhao D, Yin G, et al. Effect of SIS block copolymers on damping properties of natural rubber/AO-80 and the performance enhancement mechanism: experimental study and molecular dynamics simulation. *Colloids Surfaces A Physicochem Eng Asp* 2023;672:131705. DOI
27. He Q, Xu ZD, Xu Y, et al. Mechanical and damping properties analyses of small molecular modifiers/nitrile-butadiene rubber composite: molecular dynamics simulation. *Macromol Theory Simul* 2023;32:2200051. DOI
28. Yin C, Zhao X, Zhu J, Hu H, Song M, Wu S. Experimental and molecular dynamics simulation study on the damping mechanism of C5 petroleum resin/chlorinated butyl rubber composites. *J Mater Sci* 2019;54:3960-74. DOI
29. Zhu J, Zhao X, Liu L, Song M, Wu S. Quantitative relationships between intermolecular interaction and damping parameters of irganox-1035/NBR hybrids: a combination of experiments, molecular dynamics simulations, and linear regression analyses. *J Appl Polymer Sci* 2018;135:46202. DOI
30. Qiao B, Zhao X, Yue D, Zhang L, Wu S. A combined experiment and molecular dynamics simulation study of hydrogen bonds and free volume in nitrile-butadiene rubber/hindered phenol damping mixtures. *J Mater Chem* 2012;22:12339-48. DOI
31. Jiang Z, Wang F, Yin J, et al. Vibration damping mechanism of CuAlMn/polymer/carbon nanomaterials multi-scale composites. *Compos Part B Eng* 2020;199:108266. DOI
32. Wang F, Li L, Tang H, Wang X, Hu Y. Damping of aluminum-matrix composite reinforced by carbon nanotube: multiscale modeling and characteristics. *Sci China Technol Sci* 2023;66:1062-74. DOI
33. Duan K, Li L, Hu Y, Wang X. Damping characteristic of Ni-coated carbon nanotube/copper composite. *Mater Des* 2017;133:455-63. DOI
34. Kim SY, Park HS. Utilizing mechanical strain to mitigate the intrinsic loss mechanisms in oscillating metal nanowires. *Phys Rev Lett* 2008;101:215502. DOI PubMed
35. Song M, Yue X, Chang C, Cao F, Yu G, Wang X. Investigation of the compatibility and damping performance of graphene oxide grafted antioxidant/nitrile-butadiene rubber composite: insights from experiment and molecular simulation. *Polymers* 2022;14:736. DOI PubMed PMC
36. Hu K, Yu C, Yang Q, Chen Y, Chen G, Ma R. Multi-scale enhancement mechanisms of graphene oxide on styrene-butadiene-styrene modified asphalt: an exploration from molecular dynamics simulations. *Mater Des* 2021;208:109901. DOI
37. Liu X, Song M, Wang H, Chen S, Zheng W, Wang X. Hydrogen bond networks and wrinkles in graphene oxide/nitrile butadiene rubber composites for enhancement of damping capability: molecular simulation and experimental study. *Compos Sci Technol* 2023;240:110083. DOI
38. Wei X, Meng Z, Ruiz L, et al. Recoverable slippage mechanism in multilayer graphene leads to repeatable energy dissipation. *ACS Nano* 2016;10:1820-8. DOI
39. Zhang M, Wang X, Zhou M, Zhai Z, Jiang B. The effect of self-resistance electric heating on the interfacial behavior of injection molded carbon fiber/polypropylene composites through molecular dynamics analysis. *Polymer* 2020;207:122915. DOI
40. Rappe AK, Casewit CJ, Colwell KS, Goddard III WA, Skiff WM. UFF, a full periodic table force field for molecular mechanics and molecular dynamics simulations. *J Am Chem Soc* 1992;114:10024-35. DOI
41. Dyer T, Thamwattana N, Jalili R. Modelling the interaction of graphene oxide using an atomistic-continuum model. *RSC Adv* 2015;5:77062-70. DOI

42. Stauffer D, Dragneva N, Floriano WB, et al. An atomic charge model for graphene oxide for exploring its bioadhesive properties in explicit water. *J Chem Phys* 2014;141:044705. DOI
43. Zhang M, Liu B, Luan Y, et al. Nano-level insights on the interfacial wettability of graphene oxide-coated carbon fiber/epoxy composite. *J Mater Sci* 2023;58:8815-32. DOI
44. Tam LH, Jiang J, Yu Z, Orr J, Wu C. Molecular dynamics investigation on the interfacial shear creep between carbon fiber and epoxy matrix. *Appl Surf Sci* 2021;537:148013. DOI
45. Li B, Chen J, Lv Y, Huang L, Zhang X. Influence of humidity on fatigue performance of CFRP: a molecular simulation. *Polymers* 2020;13:140. DOI PubMed PMC
46. Zhang M, Jiang B, Chen C, Drummer D, Zhai Z. The effect of temperature and strain rate on the interfacial behavior of glass fiber reinforced polypropylene composites: a molecular dynamics study. *Polymers* 2019;11:1766. DOI PubMed PMC
47. Plimpton S. Fast parallel algorithms for short-range molecular dynamics. *J Comput Phys* 1995;117:1-19. DOI
48. Zhang H, Zhao Y, Meng T, Shah SP. The modification effects of a nano-silica slurry on microstructure, strength, and strain development of recycled aggregate concrete applied in an enlarged structural test. *Constr Build Mater* 2015;95:721-35. DOI
49. Wang G, Dai Z, Wang Y, et al. Measuring interlayer shear stress in bilayer graphene. *Phys Rev Lett* 2017;119:036101. DOI
50. Kunal K, Aluru NR. Akhiezer damping in nanostructures. *Phys Rev B* 2011;84:245450. DOI
51. Harrison JA, White CT, Colton RJ, Brenner DW. Molecular-dynamics simulations of atomic-scale friction of diamond surfaces. *Phys Rev B Condens Matter* 1992;46:9700-8. DOI PubMed
52. Granick S. Motions and relaxations of confined liquids. *Science* 1991;253:1374-9. DOI PubMed
53. Gong L, Kinloch IA, Young RJ, Riaz I, Jalil R, Novoselov KS. Interfacial stress transfer in a graphene monolayer nanocomposite. *Adv Mater* 2010;22:2694-7. DOI
54. Wang ZJ, Ma TB, Hu YZ, Xu L, Wang H. Energy dissipation of atomic-scale friction based on one-dimensional Prandtl-Tomlinson model. *Friction* 2015;3:170-82. DOI
55. Yuan R, Li P, Chen L, et al. Effects of grafting oxygen atoms on the tribological properties of graphene: molecular dynamics simulation and experimental analysis. *Appl Surf Sci* 2020;528:147045. DOI
56. Lu W, Qin F, Zhang Q, et al. Engineering foam skeletons with multilayered graphene oxide coatings for enhanced energy dissipation. *Compos Part A Appl Sci Manuf* 2020;137:106035. DOI
57. Lu W, Zhang Q, Qin F, et al. Hierarchical network structural composites for extraordinary energy dissipation inspired by the cat paw. *Appl Mater Today* 2021;25:101222. DOI